Catalytic performance of Ni-Cu/Al2O3 for effective syngas production by methanol steam reforming

Khzouz, Martin; Du, Shangfeng; Wood, Joseph; Gkanas, Evangelos

DOI:
10.1016/j.fuel.2018.06.025

Catalytic Performance of Ni-Cu/Al_2O_3 for Effective Syngas Production by Methanol Steam Reforming

Martin Khzouz[1*], Evangelos I. Gkanas[1], Shangfeng Du[2], Joe Wood[3]

1. *Hydrogen for Mobility Lab, Institute for Future Transport and Cities, Coventry University, Priory Street, Coventry CV1 5FB, United Kingdom.*
2. *School of Chemical Engineering, University of Birmingham, Edgbaston, Birmingham B152TT, UK*
3. *Catalysts and Reactions Group, School of Chemical Engineering, The University of Birmingham, Edgbaston B15 2TT, UK*

**Email:ac2127@coventry.ac.uk*

Abstract

This work investigates the catalytic performance of bimetallic Ni-Cu/Al_2O_3 catalysts for syngas production by methanol steam reforming. The synthesis and characterization of a series of Ni_x-Cu_y/Al_2O_3 catalysts with various stoichiometric fractions (x= 10, 7, 5, 3 and 0wt% and y= 0, 3, 5, 7 and 10wt% to Al_2O_3 support, respectively) are investigated and discussed. The catalytic performance is evaluated experimentally at temperature range of 225-325°C. Both mono-metallic catalyst (10wt.%Cu/Al_2O_3 and 10wt.%Ni/Al_2O_3) and bi-metallic catalysts (7wt.%Cu-3wt.%Ni/Al_2O_3, 5wt.%Cu-5wt.%Ni/Al_2O_3 and 3wt.%Cu-7wt.%Ni/Al_2O_3) are synthesized using an impregnation method and characterized by means of SEM, temperature programmed reduction (TPR), BET analysis, XRD and TGA. It is found that the bimetallic Ni-Cu catalyst had a strong influence on the amount of CO_2 and CO produced due to the different selectivity towards the water gas shift reaction and methanol decomposition reaction. The increase of the Ni content leads to an increase in CO and decrease in CO_2 yields. The bimetallic catalyst did not produce CH_4, revealing that Cu alloying in Ni catalyst had an inhibiting effect for CO and/or CO_2 hydrogenation.

1. Introduction

Methanol is being used as source of fuel to produce syngas in small scale reformers [1]. The conversion of methanol to syngas takes place over a lower temperature range of 200-325°C compared to other liquid fuels such as ethanol which is only converted at temperatures above 500 °C. The absence of C-C bonds in methanol leading to low energy chemical bonds makes the reforming of methanol popular for the development of fuel processor for hydrogen production and electricity generation using fuel cells [2, 3].

The steam reforming of methanol (Eq. 1) ideally produces dry gases consisting of 75 vol% of hydrogen and 25 vol% carbon dioxide with complete stoichiometry conversion [4, 5]. The methanol steam reforming process (Eq. 1) [6-10] is represented by summation of decomposition reaction of methanol (Eq. 2) and water gas shift reaction (Eq. 3) [7, 11, 12]. According to the stoichiometry of the reactions, complete steam reforming of methanol notwithstanding equilibrium limitations is predicted using highly active and selective catalyst to produce hydrogen and carbon dioxide at a reforming temperature of (200-300°C) and at atmospheric pressure [7, 11, 12].

$$CH_3OH + H_2O \rightleftharpoons CO_2 + 3H_2 \qquad \Delta H°_{298} = +49.5 \text{ kJ/mol} \qquad \text{(Eq. 1)}$$

$$CH_3OH \rightleftharpoons CO + 2H_2 \qquad \Delta H°_{298} = +90.2 \text{ kJ/mol} \qquad \text{(Eq. 2)}$$

$$CO + H_2O \rightleftharpoons CO_2 + H_2 \qquad \Delta H°_{298} = -41.0 \text{ kJ/mol} \qquad \text{(Eq. 3)}$$

The bimetallic effect of catalyst for methane steam reforming was studied [13-15].Ni-Cu based catalysts were discussed in the literature for steam reforming of both ethanol [16-18] and methanol [19-21]. Ni-Cu supported on carbon nanotubes have been studied recently[19]and it was observed that alloy Ni with Cu could weaken the adsorption between Ni and hydrogen thus enhancing the catalyst activity due to the increase of methanol contact with Ni particles.

Ni_xCu_y-Al catalysts were also synthesised with different Ni-Cu contents [20].The results showed that NiCu alloy had improved catalyst performance compared to the monometallic Cu for methanol and ethanol reforming. It was also demonstrated that the introduction of Cu in the catalyst formulation suppresses coke deposition and the sintering of the active phase in steam reforming. The addition of Cu revealed a positive effect by preventing the formation of methane with enhanced stability. The experiment was conducted by constant increase of the reaction temperature. However, it cannot prove

whether the formation of CH_4 from hydrogenation reaction was supressed as the temperature was increasing during the experiment, for which a study under steady operation conditions was required.

We also studied 5%Ni-5%Cu/Al_2O_3 previously by comparison with two commercial catalysts: Ni/Al_2O_3 and Cu/ZnO/Al_2O_3[21]. It was shown that Cu increased the active particle size of Ni compared to Ni/Al_2O_3 and Ni improved Cu dispersion compared to Cu/ZnO/Al_2O_3 catalyst. The bimetallic catalyst with 5%Ni-5%Cu/Al_2O_3 proved to be very active both in methane and methanol steam reforming compared with commercial catalysts.

In the current work, we systematically investigated the bimetallic catalytic activity by performing reaction conditions for four hours in order to study the gas mixture composition under constant reaction temperature and stable operation conditions. The main problem that this work intends to answer is the effect of the metallic/alloy phase of the catalysts with different loadings on the catalytic performance towards syngas production. Thus, the reaction yields and pre and post characterisation of the catalysts are investigated for mono-metallic, bimetallic and physical mixture of single metal catalysts.

Various loadings of bimetallic, 7wt.%Cu-3wt.%Ni/Al_2O_3, 5wt.%Cu-5wt.%Ni/Al_2O_3 and 7wt.%Ni-3wt.%Cu/Al_2O_3 catalysts were synthesized using impregnation method and characterized by different techniques. The results were compared with the monometallic 10wt.%Cu/Al_2O_3 and 10wt.%Ni/Al_2O_3 catalysts.

2.1 Catalyst preparation

The Ni_x-Cu_y/Al_2O_3 catalyst was synthesised via an impregnation method. Both mono-metallic catalysts, 10wt.%Cu/Al_2O_3 and 10wt.%Ni/Al_2O_3, and bi-metallic catalysts (7wt.%Ni-3wt.%Cu/Al_2O_3, 5wt.%Ni-5wt.%Cu/Al_2O_3 and 3wt.%Ni-7wt.%Cu/Al_2O_3) were prepared. Nickel nitrate ($Ni(NO_3)_2.6H_2O$) and/or copper nitrate ($Cu(NO_3)_2.3H_2O$) provided commercially (Fisher Scientific) were dissolved in high purity ethanol (99.8%) using a magnetic stirrer. To ensure good mixing and dissolution, the mono-metal solution was mixed for 30 minutes. However, for the bi-metallic catalyst type, a copper metal solution was prepared by mixing the solution for 30 minutes, then nickel nitrate was added to the prepared solution and it was further mixed for 30 minutes. To the above-prepared nitrate metal solution, 6 grams of trilobe Al_2O_3 supplied by Johnson Matthey were added and mixed for

two hours using an ultrasonic mixer/heating bath (Bandelin Sonorex bath) set at a temperature of 27°C. The catalyst was dried overnight in a static oven at 100°C. In the final preparation stage the catalyst was heated for calcination to 500°C at rate of 5°C/min, held at that temperature for 5 hours, then finally cooled at rate 5°C/min to ambient room temperature.

The prepared mono-metallic and bi-metallic catalysts in the rest of this work will be denoted as 10%Cu, 10%Ni , 7%Ni-3%Cu, 5%Ni-5%Cu and 3%Ni-7%Cu for brevity.

2.2 Catalyst characterization

The catalysts were characterized using Scanning Electron Microscope (SEM), nitrogen adsorption-desorption cycles analysed by the Brunauer Emmett Teller (BET) method to determine surface area, Temperature Programmed Reduction (TPR), X-ray Diffraction (XRD) and Thermo Gravimetric Analyses (TGA).

A Philips XL-30 with LaB6 filament SEM fitted with an Oxford Instruments INCA Energy Dispersive X-ray Spectroscopy (EDS) system was used to study the catalyst morphology and composition for both fresh and spent catalysts. The SEM apparatus uses a NordlysS camera which is able to produce images with minimal geometric distortion at a resolution of 1344x1024 pixels. The SEM captures adjusted angle from 15°-130° upon a 50x50 mm stage. The scanned samples were coated with gold before being introduced to the microscope chamber. The external morphology of the samples was recorded in the range of 1 µm up to 100 µm and a two-dimensional image was displayed on the computer screen using INCA software.

In order to determine the catalyst surface area and average pore size for fresh and spent catalysts, the samples were analysed by the nitrogen adsorption-desorption method. The measurements were carried out over approximately 1.4g of catalyst sample using a Micrometrics ASAP 2010 analyser. Accelerated Surface Area and Porosimetry (ASAP) use the static volumetric technique to determine surface area using N_2physisorption isotherms at -196°C. The volume of gas adsorbed was recorded by the instrument. Then the experiment data collected was used to calculate the BET surface area and average pore size[22].

The TPR runs were conducted using a Micrometrics AutoChem 2920 Analyzer on 1g fresh catalyst ground by pestle and mortar. The catalyst sample was pretreated using argon as preparation gas at flow rate 50 ml/min for cleaning the entire lines of the apparatus. The sample was pretreated by increasing the temperature up to 500°C at 10°C/min and held for one hour in order to remove any moisture from the sample and tube, then the sample was cooled down to ambient temperature. After that, 10%H_2/90%Ar at flow rate of 50 ml/min was introduced and the temperature was increased to 900°C at 10°C/min to record hydrogen uptake using Thermal Conductivity Detector (TCD) [23].

The XRD characterization was performed using a Bruker D8 Advanced Diffractometer. The catalyst was crushed using a mortar and pestle in order to obtain a powder of the catalyst then it was scanned and recorded at room temperature in the two theta range from 30° to 90°, with 0.02° step size and Cu$K\alpha$ radiation, λ=0.154 nm and K=0.9. The XRD patterns were assigned according to the XRD database (PDF-4+2012) provided by International Centre for Diffraction Data (ICDD).

A TGA was carried out using a NETZSCH TG 209 F1 instrument [24]. The mass of the used catalyst was monitored against the programmed temperature in order to study the mass changes of carbon formed on the used catalyst [25].The amount of carbon formation on the catalyst after the reaction for all operated catalysts at 225-325°C and S/C (steam to carbon ratio) of 1.7 was achieved by introducing air (50 ml/min) into 20 mg of the spent sample and heating the sample from 25°C to 900°C at a ramp rate of 10°C/min. Then, the catalyst selectivity for solid carbon (Sel_C) was estimated as shown in Eq. 4.

$$Sel_C\ (\%) = 100 \times \frac{n_{carbon}}{n_{CH3OH,in}} \qquad \text{(Eq. 4)}$$

Where n_i *is total moles for reaction duration for species* i (mol).

2.3 Catalytic reactivity test

The methanol steam reforming reaction was investigated in terms of reaction conditions, fuel conversion and the amount of H_2, CO_2,CO and CH_4 produced. Fig. 1 presents the experimental rig used for the current study. The rig consists of three modules; the feed, reactor and gas analysis modules. The

feeding module is composed of a Cole-palmer EW-74930-05 series one pump which can supply water-methanol premix to the vaporization zone and reactor. A vaporizer constructed from trace heating tape (OMEGA FGR-100) wrapped around the feed pipe is used to generate steam at 110°C, the temperature of which was controlled using a West 2300 PID controller. Digital Brooks mass flow controllers were used to control the flow rate of the various gases fed to the reactor during the catalytic tests. The reactor module consists of a high temperature furnace (Severn Thermal Solutions Ltd.). Inside the furnace, the fixed bed reactor was constructed of stainless steel tube (316L) with inner diameter 10.9 mm, wall thickness 0.89 mm and tube length of 395 mm. 3g catalyst was packed into the reactor and the void space above and below was filled with glass beads; the catalyst bed height was 50mm. The temperature of the reactor was measured using a K type thermocouple fixed near the centre of the bed. The reformate stream at the outlet of the reactor was cooled before proceeding for gas analysis. Therefore, a condenser facilitated by ice cubes in a bath surrounding a coiled section of the reactor outlet pipe at a temperature of -2°C was used. After cooling, the unreacted liquid was separated from gaseous stream in a specially designed gas-liquid separator unit. The various gases generated in the reaction were analysed using a Refinery Gas Analyzer (RGA). The reformate gases were sampled using an online connection to Agilent 7890A model gas analyzer. The gas sample duration was five minutes before the generated gas was withdrawn out to the vent.

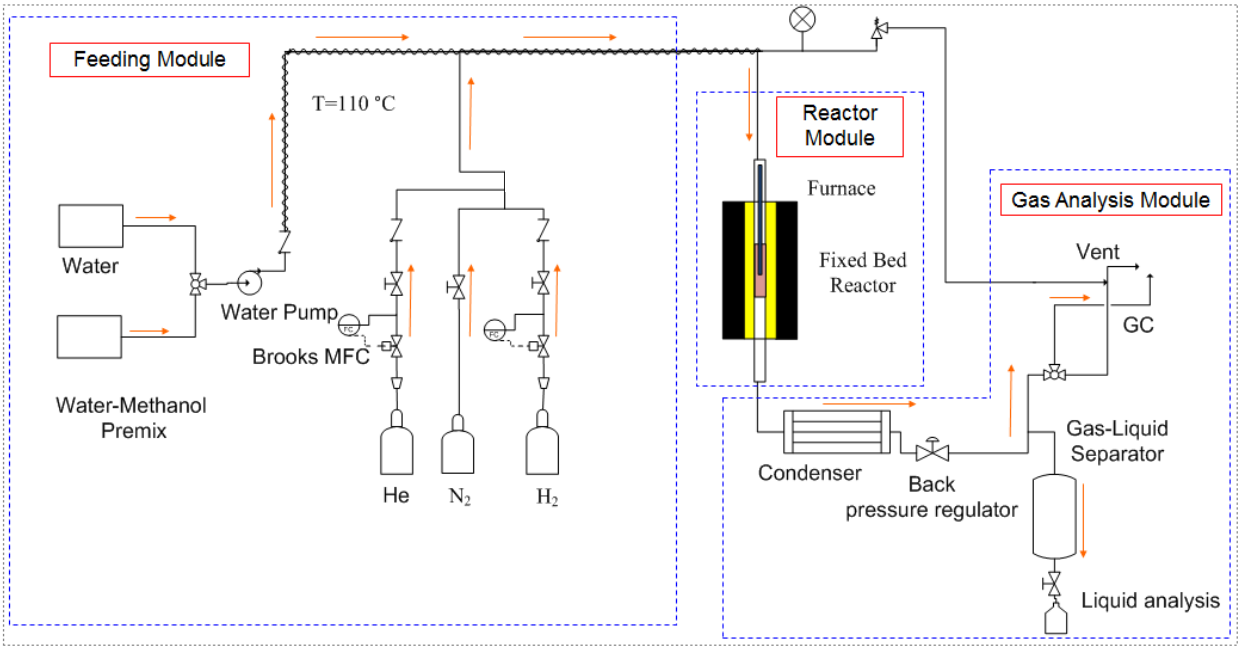

Fig. 1.Experimental test rig flow sheet diagram.

Before the reaction commenced, the system was purged with N_2 for five minutes to remove the air from the pipes and reactor bed. Then, hydrogen at flow rate of 10 ml/min was introduced to reduce the catalyst at its reduction temperature determined from TPR (Fig.6), the TPR profile revealed that 10%Cu could be reduced at 250°C, 10%Ni at 650°C, 7%Cu-3%Ni at 350°C, 5%Cu-5%Ni at 380°C and 7%Ni-3%Cu at 425°C. The reduction process was carried out by raising the temperature to its target point at a rate of 5°C/min and maintaining it for 30 minutes in hydrogen flow before switching to pure N_2 for purging. Methanol steam reforming was carried out at temperatures of 225, 250, 275, 300 and 325°C in order to study the catalyst reactivity and methanol conversion. Distilled water mixed with pure methanol (99.99%) in a specific mole ratio of 1.7 was injected using the pump at constant flow rate of 0.06 ml/min. Then, the reactor was left for one hour in order for the temperature to stabilize under the reaction conditions. Once stable operation was achieved, samples were withdrawn for gas analysis, which was repeated every 15 minutes and recorded for 3 hours run duration of the catalyst reactivity test. The output flow rate was measured manually using bubble flow meter and stopwatch to calculate the flow rate of reformate.

In order to study conversions and products yields; an elemental analysis (carbon and hydrogen balance) using reactor exit concentrations of CO, CO_2, CH_4 and H_2 and the inlet flow of methanol was performed. The unmeasured amount of H_2O was calculated. The carbon balance Eq. 5 contains two unknowns, $\dot{n}_{out,dry}$, $\dot{n}_{CH_3OH,out}$.

$$\left(y_{CO} + y_{CO_2} + y_{CH_4}\right) \times \dot{n}_{out,dry} + 1 \times \dot{n}_{CH_3OH,out} = 1 \times \dot{n}_{CH_3OH,in} \quad \text{(Eq. 5)}$$

$y_i = mol\ \ fraction\ \ of\ \ species\ \ i.$

$\dot{n} = total\ \ molar\ \ flow\ \ rate\ \ (mol/\min)$

$\dot{n}_i = molar\ \ flow\ \ rate\ \ of\ \ species\ \ i\ \ (mol/\min)$

where, in and out subscriptsdenote relevant mol entering or leaving the reaction.

The hydrogen balance analysis was performed as shown in Eq. 6. Hydrogen entering the reaction from water and methanol equals the hydrogen leaving the reaction. The Eq. 6 contains three unknowns, $\dot{n}_{out,dry}$, $\dot{n}_{H_2O,out}$ and $\dot{n}_{CH_3OH,out}$

$$\left(2y_{H_2} + 4y_{CH_4}\right) \times \dot{n}_{out,dry} + 2 \times \dot{n}_{H_2O,out} + 4 \times \dot{n}_{CH_3OH,out} = 4 \times \dot{n}_{CH_3OH,in} + 2 \times \dot{n}_{H_2O,in} \quad \text{(Eq. 6)}$$

$y_i = mol\ \ fraction\ \ of\ \ species\ \ i.$

$\dot{n}\ = total\ \ molar\ \ flow\ \ rate\ \ (mol/\min)$

$\dot{n}_i = molar\ \ flow\ \ rate\ \ of\ \ species\ \ i\ \ (mol/\min)$

From the above elemental analysis, the unknown $\dot{n}_{out,dry}$ was measured in the experiment from bubble meter after water condensation, $\dot{n}_{CH_3OH,out}$ and $\dot{n}_{H_2O,out}$ were calculated.

The conversions for methanol and water were obtained by Eq.7-8:

$$x_{CH_3OH} = \frac{\dot{n}_{CH_3OH,in} - \dot{n}_{CH_3OH,out}}{\dot{n}_{CH_3OH,in}} \quad \text{(Eq. 7)}$$

$$x_{H_2O} = \frac{\dot{n}_{H_2O,in} - \dot{n}_{H_2O,out}}{\dot{n}_{H_2O,in}} \quad \text{(Eq. 8)}$$

The molar flow rates of products from the reaction were calculated by:

$$\dot{n}_{i,out} = y_i \times \dot{n}_{out,dry} \quad \text{(Eq. 9)}$$

The products yields for hydrogen, carbon dioxide and carbon monoxide were obtained in mol/min per mol/min of methanol as shown in Eq.10-12:

$$H_2 yield = \frac{\dot{n}_{H_2,out}}{\dot{n}_{CH_3OH,in}} \quad \text{(Eq. 10)}$$

$$CO_2 yield = \frac{\dot{n}_{CO_2,out}}{\dot{n}_{CH_3OH,in}} \quad \text{(Eq. 11)}$$

$$CO\ yield = \frac{\dot{n}_{CO,out}}{\dot{n}_{CH_3OH,in}} \quad \text{(Eq. 12)}$$

3. Results and Discussion

3.1 Catalytic reactivity test

The catalytic reactivity measurement was performed over a temperature range of 225-325°C, with the S/C ratio of 1.7 and liquid hourly space velocity of 0.77h^{-1}. The methanol and water conversions are displayed in Fig. 2. The bimetallic catalyst revealed a lower water conversion than 10%Cu catalyst at all operating temperatures and showed a superior methanol conversion at 300-325°C. For 7%Cu-3%Ni catalyst, the methanol conversion decreased from 94% at 225°C to 90% at 275°C, then it showed an increase up to 98.5% at 325°C. The 7%Cu-3%Ni catalyst revealed a slight increase in water conversion within 225-275°C then it decreased rapidly within 300-325°C. The slight increase in water consumption indicates that methanol steam reforming is a part of the reaction. However, the water consumption was less than in 10%Cu catalyst for all temperatures which explains the existence of decomposition reaction as explained later from the amount of CO produced. Both 5%Cu-5%Ni and 3%Cu-7%Ni catalysts showed an increase in methanol conversion with increasing the reaction temperature (87.6%-97.8% for 5%Cu-5%Ni and 76.8-95.9% for 3%Cu-7%Ni) which is explained by the possible methanol decomposition reaction that occurs on Ni species in bimetallic catalyst where a lot of CO was observed. The water consumption for 5%Cu-5%Ni was less than 10%Cu and it decreased with increasing the reaction temperature. There was no water consumption for 3%Cu-7%Ni, this explains the low methanol conversion at low reaction temperature (225-250°C) since the methanol decomposition reaction is the dominant and the conversion increase with increasing the reaction temperature.

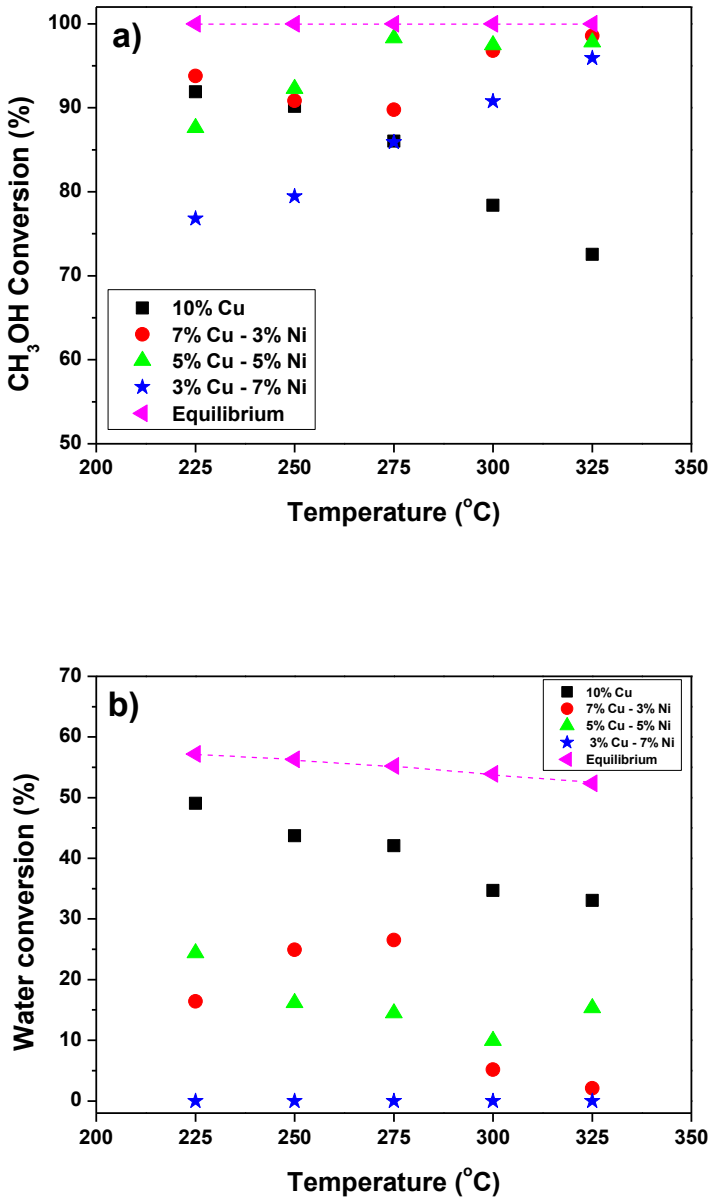

Fig. 2. Methanol and water conversion with S/C of 1.7 for 10%Cu, 7%Cu-3%Ni, 5%Cu-5%Ni and 3%Cu-7%Ni methanol catalysts: (a) methanol conversion and (b) water conversion

The steam reforming reaction showed that 10%Cu produced the highest amount of hydrogen within 225-300°C compared to other prepared catalysts, as shown in Fig. 3a. It was noticed that adding Ni metal to the Cu catalyst reduced the amount of hydrogen produced and showing that the bimetallic catalyst is less selective for hydrogen production than the monometallic Cu catalyst at such an operating temperature. The hydrogen yield of 2.2 mol/mol-CH_3OH was observed for the 5%Cu-5%Ni catalyst at 325°C which is the highest amount for bimetallic catalyst at such temperature. The hydrogen yield was approximately constant (2.0-2.2 mol/mol-CH_3OH) for 7%Cu-3%Ni and 5%Cu-5%Cu

catalysts. The hydrogen yield increased from 1.5 mol/mol-CH_3OH at 225°C to 1.8 mol/mol-CH_3OH at 325°C for 3%Cu-7%Ni catalyst. More Ni metal in the catalyst made the catalyst less selective to hydrogen as observed for the 3%Cu-7%Ni catalyst. This confirms that Ni rich catalysts (with more than 5wt.%) are favourable for the decomposition reaction rather than the steam reforming reaction itself. For bimetallic catalyst, the decrease in hydrogen amount compared to 10%Cu could be due to the active methanol decomposition reaction over Ni and the reverse water gas shift reaction affecting the concentration of hydrogen produced as both reactions are thermodynamically favoured at such operation temperature.

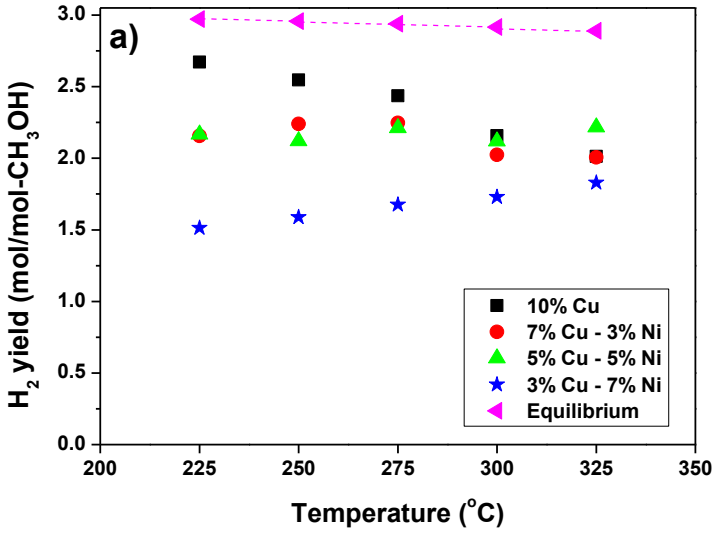

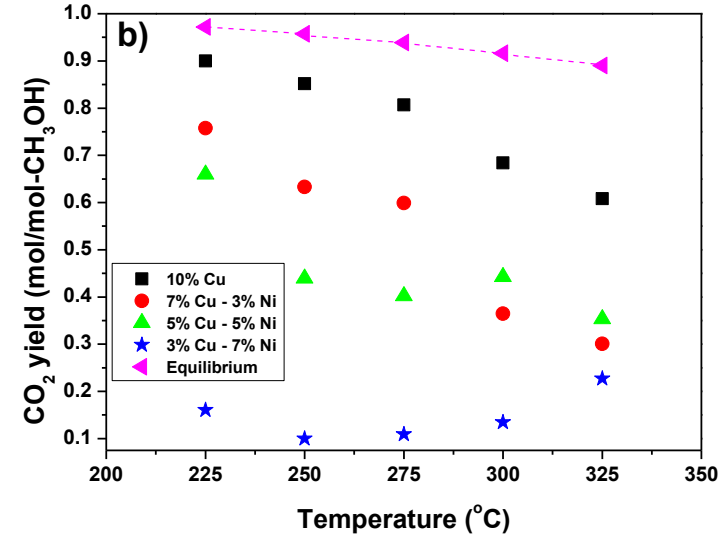

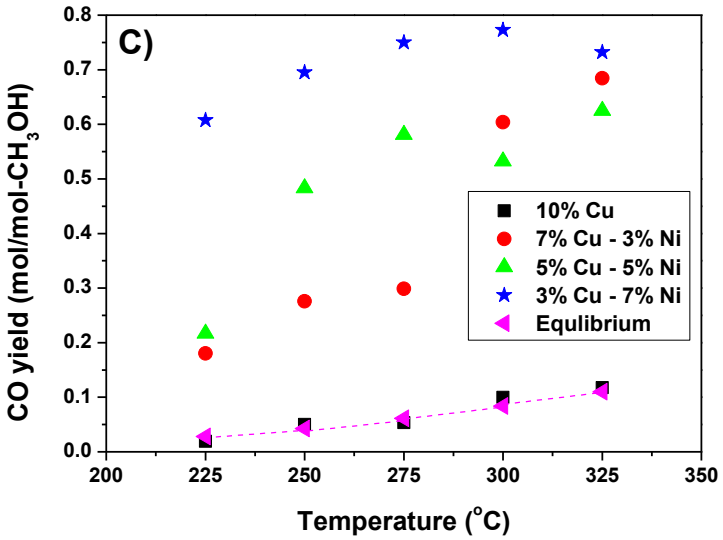

Fig. 3. H_2, CO_2 and CO yields within 225-325°C and S/C of 1.7 for 10%Cu, 7%Cu-3%Ni, 5%Cu-5%Ni and 3%Cu-7%Ni methanol catalysts: a) H_2 yield, b) CO_2 yield and c) CO yield.

The carbon oxide yield profiles are presented in Fig. 3b and c as a function of temperature for various catalysts. The influence of increase the Ni content in the catalyst on reformate yield had shown an increase in CO and decrease in CO_2. It is observed from Fig. 3b that increasing the amount of Ni content in the catalyst affects in a negative way for CO_2 production compared to 10% Cu. The amount of CO_2 formed in operated bimetallic catalyst is less than the amount obtained with the monometallic

Cu catalyst. It was also observed that with 10%Cu, 7%Cu-3%Ni, 5%Cu-5%Ni catalysts, the amount of CO_2 decreased when increasing the temperature in the range of 225-325°C. However, the amount of CO_2 formed with 3%Cu-7%Ni decreased within 225-275°C and then increased within 300-325°C, this observation is discussed later. From Fig. 3c, the amount of CO produced increased with the increase of Ni content upon the catalyst. The trend in CO yield with catalyst type is opposite to the trend of CO_2 shown in Fig. 3b.

In order to understand the effect of the Ni content, methanol steam reforming over 10% Ni catalyst was tested. The main products over 10% Ni (Table 1) were CO and H_2, which were produced from the methanol decomposition reaction. The formation of a small amount of CO_2 is related to the water gas shift reaction. The methanol steam reforming over 10%Ni produced a significant amount of CH_4 due to CO and CO_2 hydrogenation which was not observed in 10%Cu and bimetallic Ni-Cu catalysts. The difference between 10%Ni catalyst and 10%Cu catalyst is that the latter one promotes the water gas shift reaction as observed from the formation of large quantities of CO_2 and small quantities of CO in Fig. 3b and c, respectively. As a result, the water gas shift reaction equilibrium shifts towards the reactants with increasing the temperature at which the conversion of CO to CO_2 is decreased as observed for 10% Cu in Fig. 3b.

The bimetallic effect for Ni-Cu catalyst was also compared with the physical mixture of single metal 10%Cu and 10% Ni catalysts (Table 1). The reaction over the physical mixture of single metal 10%Ni and 10% Cu (Table 1) showed significant formation of CH_4 which was not observed for 10% Cu and Ni-Cu catalysts. Copper-based catalysts have good activity for the water gas shift reaction, and have no methanation activity. The existence of single Ni catalyst in the reactor promotes CH_4 formation by CO and CO_2 hydrogenation. The reaction over physical mixture of catalyst showed less CO and more CO_2 than the bimetallic catalytic system. This indicates that the 10%Cu catalyst in the physical mixture of catalyst controls the high activity of the water gas shift reaction.

Table 1. Product yield for methanol reaction for 10%Ni and for physical mixture of single metal 10%Cu and 10%Ni catalysts.

	Temperature (°C)	**Conversion (%)**		**Yield (mol/mol CH_3OH)**			
		CH_3OH	**H_2O**	**H_2**	**CO_2**	**CO**	**CH_4**

10%Ni	325	70.9	15.0	1.47	0.11	0.50	0.10
10%Ni, 10%Cu*	325	96.1	22.5	2.08	0.71	0.13	0.11
10%Ni, 10%Cu*	300	91.6	15.3	1.84	0.68	0.14	0.09
10%Ni ,10%Cu*	275	86.9	27.0	2.03	0.72	0.11	0.03

*Physical mixture of single metal (1.5 g of 10%Cu and 1.5 g of 10%Ni).

By comparing the carbon oxide yield over monometallic 10%Cu, 10%Ni and physical mixture of single metals 10%Cu and 10%Ni catalysts, it was observed that the CO amount is strongly dependent on the Cu content in the bimetallic Ni-Cu catalysts, which affects the water gas shift reaction equilibrium. The decrease in Cu content with respect to Ni in the catalyst showed an increase in CO formation, suggesting that the water gas shift reaction moves towards reactants. The increase in Ni content with respect to Cu on the bimetallic catalyst revealed additional CO derived from the methanol decomposition reaction. The bimetallic Ni-Cu catalyst did not produce CH_4,suggesting an inhibiting effect of Cu alloying for CO and CO_2 hydrogenation on Ni. Hence, that Cu has a low CO dissociation activity where CO remains on the catalyst surface. As a result, the Cu presented in Ni-Cu catalyst prevents the CO activation on Ni sites in Ni-Cu catalyst.

The reaction activity profile (Fig. 3b and Fig. 3c) for carbon oxide yield for 3%Cu-7%Ni revealed slightly different trends over 5%Ni-5%Cu and 7%Cu-3%Ni catalysts. The amount of CO_2 formed with 3%Cu-7%Ni decreased within 225-275°C then increased at temperatures in the range of 300-325°C. The Cu promotes the water gas shift reaction at low temperature and the reaction equilibrium moves towards the reactants by increasing the temperature. Hence, the CO amount will increase. On the other hand, Ni promotes methanol decomposition reaction and the reaction becomes very operative with increasing the temperature. Accordingly, it is expected that the amount of CO would increase and CO_2 decrease with increasing the reaction temperature as observed for 5%Ni-5%Cu and 7%Cu-3%Ni catalysts. Indeed, the reverse water gas shift reaction was found to be active at temperatures of 300-325°C for 7%Cu-3%Ni and 5%Cu-5%Ni catalysts, evidenced by a drop in water consumption (Fig. 2b.) at these high temperatures. For 3%Cu-7%Ni catalyst, the Ni rich alloy effect was observed. The Ni-Cu alloy phase is responsible for balancing the amount of CO with respect to CO_2.

In summary, a higher metal content of Ni over Cu has a strong influence upon the amount of CO_2 by controlling the dominant reaction paths. When increasing the amount of Ni, the effect of bimetallic Ni-Cu becomes dominant in the reaction. The decomposition reaction on the metallic phase of Ni-Cu is responsible for producing a high amount of CO in the products. From the above results, the decomposition reaction of methanol occurs predominantly on the metallic phase of Ni-Cu and the reverse water gas shift reaction occurs at the Cu site and increase with increasing the reaction temperature, where these reactions are the major contributors for the CO production. The decomposition reaction mainly transforms methanol to CO and H_2 (Eq.2) and slow water gas shift reaction converts CO to CO_2 (Eq.3), the existence of the alloy phase of metal and/or metal phase determines CO_2 and CO amount. The increasing Ni metals content had a positive effect on methanol conversion and showed a high methanol conversion at 300-325°C. The methanol conversion was high for 5%Cu-5%Ni and 7%Cu-3%Ni (98.5%) at 325°C which could possibly be explained by the active decomposition reaction. The increase of Ni metals content showed an adverse effect on the amount of hydrogen produced. Increasing the amount of Ni metals content from 3% to 7% led to a big decrease for CO_2 and an increase for CO. It is also noticed that the bimetallic Ni-Cu catalyst produced negligible amount of CH_4. It was validated experimentally in this work that performing methanol steam reforming reaction over pure 10%Ni catalyst or over physical mixture of single metal 10%Ni and 10%Cu catalysts at 325°C and S/C of 1.7 produced a noticeable amount of CH_4 (up to 0.11 mol/mol-CH_3OH). The effects of the Ni-Cu alloy phase in the reaction for all bimetallic catalysts were observed from the negligible amounts of CH_4 produced during the reaction, which means that the alloy phase is responsible for decreasing the hydrogenation effects of CO or CO_2 to produce CH_4.

3.2 Catalyst characterization

3.2.1 SEM Imaging

Fig.4 shows the SEM images for all the prepared catalysts. Fig. 4a presents the Al_2O_3 support and the variation in darkness from light grey (low aluminium concentrations) to dark grey (high aluminium concentrations). Fig.4b presents the catalyst with 10% Cu and the copper species as shaded white patches (highlighted by a marked blue circle) distributed over a light grey background of Al_2O_3 support. The estimated size of particles is 5-15 µm. The SEM image of 10%Ni/Al_2O_3 catalyst in Fig.4c shows an irregular distribution of bright white spherical species (highlighted by a marked red circle)

upon a dark grey background of Al_2O_3 with particle size of 6-12 µm. Fig.4d shows the surface morphology of 7%Cu-3%Ni/Al_2O_3 catalyst. Copper species (shaded white, highlighted by a marked blue circle) and Ni species (bright white, highlighted by a marked red circle), the approximate size of species is 6.5 µm. Performing SEM for 5%Cu-5%Ni shows that both Cu particles (shaded white, highlighted by a marked blue circle) and Ni particles (bright white, highlighted by a marked red circle) are distributed throughout the light grey of the Al_2O_3 support with approximate sizes 4.4-10.9 µm. Agglomerates of larger particle sizes (highlighted by a marked red circle) are apparent in the 7%Ni-3%Cu sample (Figure 4f) compared to 7%Cu-3%Ni (Figure 4d) and 5%Ni-5%Cu (Figure 4e) samples. Introducing additional Ni to the bimetallic system caused morphological changes compared to 7%Cu-3%Ni and 5%Ni-5%Cu samples [26]. This is related to the fact that Ni species normally reveal more agglomerates with increasing Ni concentration [27].

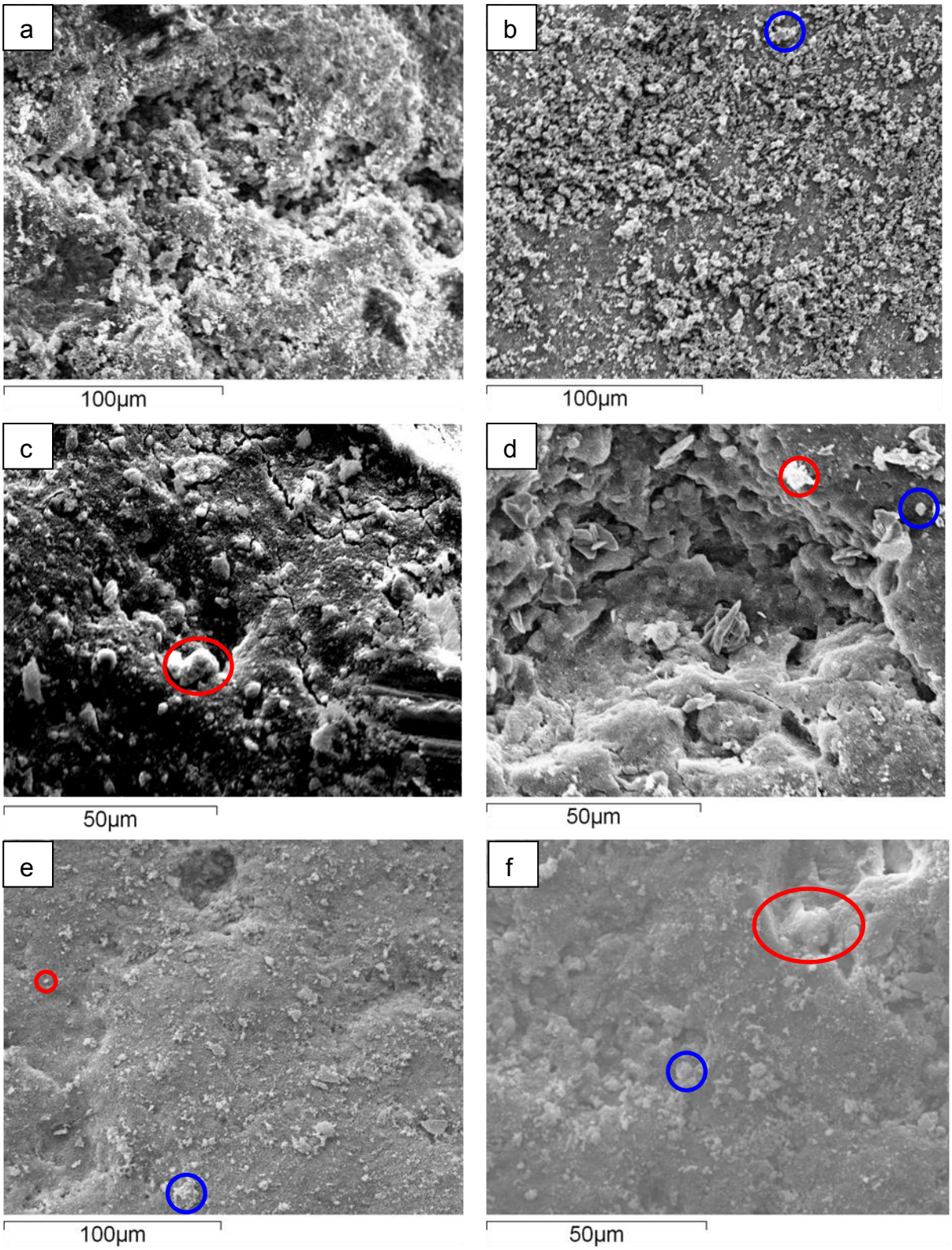

Fig.4. SEM images of the prepared catalysts: a) Al_2O_3, b) 10%Cu, c) 10%Ni, d) 7%Cu-3%Ni, e) 5%Cu-5%Ni and f) 7%Ni-3%Cu.

The morphological appearance of the prepared catalysts post the reaction (10%Cu, 7%Cu-3%Ni, 5%Cu-5%Ni and 3%Cu-7%Ni) operated at 225°C and 325°C and the S/C of 1.7 are shown in Figures 5

and 6, respectively. The SEM images of the used 10%Cu catalyst which had been previously exposed to a temperature of 225°C during reaction, depicted in Figure 5a, shows a shade of white spots which correspond to Cu species (highlighted by a marked blue circle) distributed over grey Al_2O_3 support. Small agglomerates of particles are apparent on the left side of the image (highlighted by a marked green circle). The distribution of particles showed uniformity over the support. The SEM image of the used 10%Cu catalyst reacted at 325°C in Figure 6a showed shade white spots (highlighted by a marked blue circle) which represent Cu species distributed over shades of grey Al_2O_3 support but more agglomeration (highlighted by a marked green circle) have appeared on the catalyst compared to the SEM image of the used 10%Cu catalyst reacted at 225°C. This would be explained by the fact that increasing the reaction temperature to 325°C leads to the sintering of copper crystallites, causing coarsening [28].

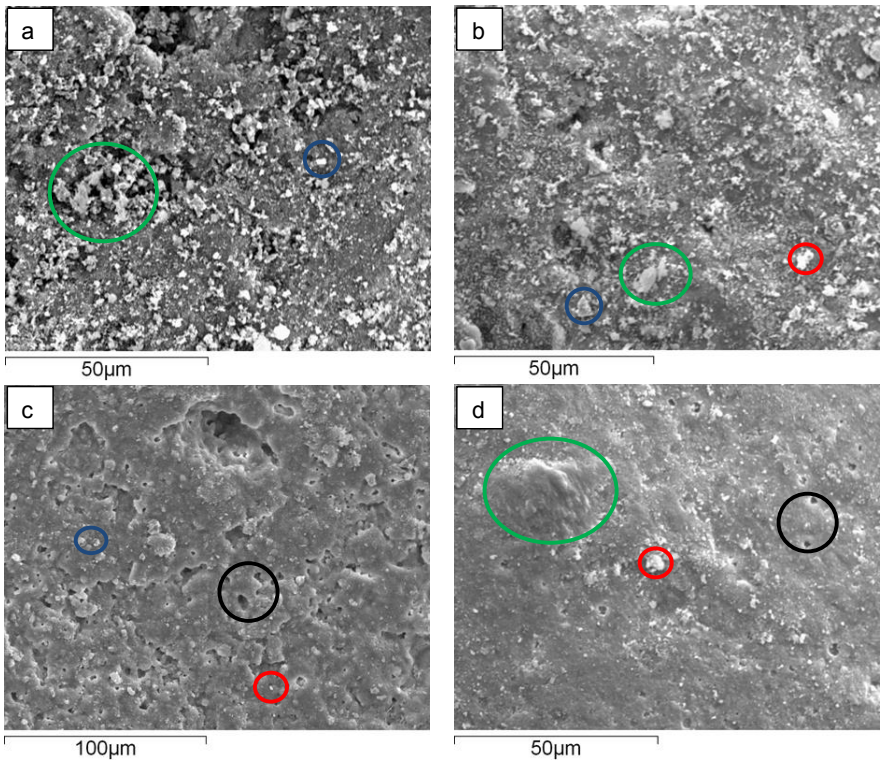

Fig.5. SEM images of the used methanol catalysts reacted at 225°C and S/C of 1.7: a) 10%Cu, b) 7%Cu-3%Ni, c) 5%Cu-5%Ni and d) 3%Cu-7%Ni.

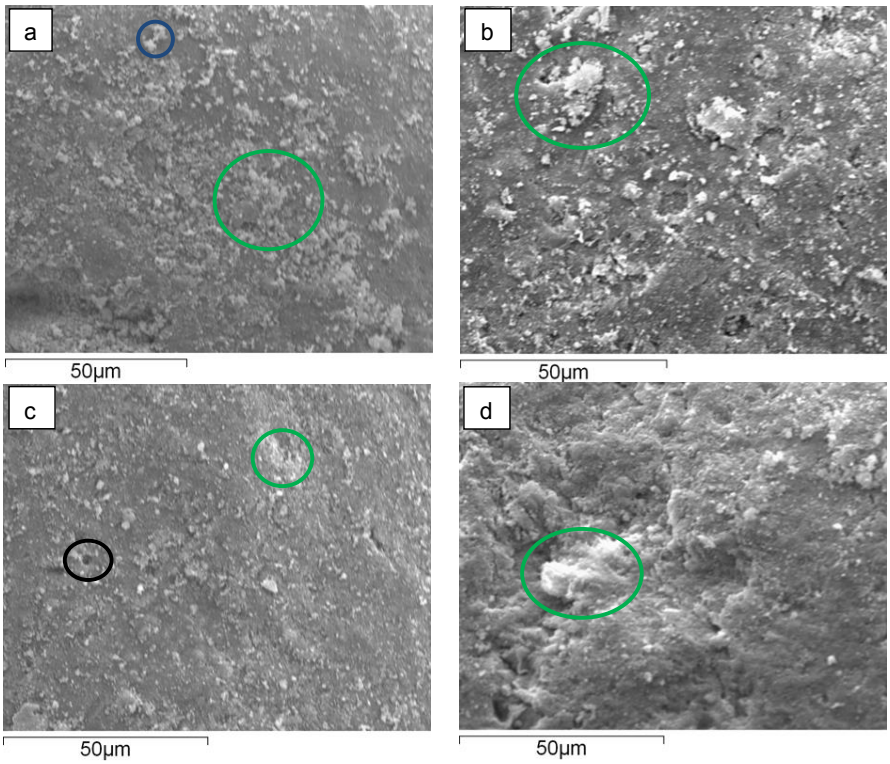

Fig.6. SEM images of the used methanol catalysts reacted at 325°C and S/C of 1.7: a) 10%Cu, b) 7%Cu-3%Ni, c) 5%Cu-5%Ni and d) 3%Cu-7%Ni.

The surface morphology of the used 7%Cu-3%Ni catalyst reacted at 225°C is showed in Figure 5b. Shades of white spots which represent Cu species (highlighted by a marked blue circle) and bright white spots which refer to Ni species (highlighted by a marked red circle) are distributed uniformly across the surface of the aluminium support with small agglomerates of particles appearing on the catalyst surface (highlighted by a marked green circle). Figure 6b shows the SEM image of the used catalyst operated at 325°C in the reaction, from which it is observed that larger agglomerates of particles appear on the catalyst surface (highlighted by a marked green circle) compared to 7%Cu-3%Ni reacted at temperature 225°C.

The SEM image of the used 5%Cu-5%Ni reacted at 225°C in Figure 5c shows shades of white spots which correspond to Cu species (highlighted by a marked blue circle) and bright white spots which represent Ni species (highlighted by a marked red circle) distributed across the surface of the Al_2O_3 support. The SEM image of the used 5%Cu-5%Ni reacted at 325°C is reported in Fig.6c. It is observed that a uniform distribution of species occurs with smaller agglomerates (highlighted by a marked green circle) compared to the used 10%Cu and 7%Cu-3%Ni catalysts reacted at 325°C. However, some

cracks (highlighted by a marked black circle) are visible for the used 5%Cu-5%Ni reacted at 225°C and 325°C.

The SEM image in Figure 5d for the used 3%Cu-7%Ni reacted at 225°C showed bright white spots which refer to Ni species (highlighted by a marked red circle) throughout the support with large agglomerates (highlighted by a marked green circle) and cracks observed on the surface (highlighted by a marked black circle). From Figure 6d, the used 3%Cu-7%Ni catalyst reacted at 325°C showed large agglomerates of bright white spots which correspond to Ni species agglomeration (highlighted by a marked green circle).

3.2.2 BET surface area

The BET surface area for fresh prepared catalyst showed that the surface area ranged from 120 m^2/g for 10%Cu to 128 m^2/g for 5%Cu-5%Ni catalyst. The surface area of trilobe alumina used as support was 142 m^2/g. Impregnated samples resulted in a lower surface area with respect to pure Al_2O_3 due to pore blockage during metal deposition. The BET surface area showed that the used catalysts had a lower surface area than the fresh catalysts as summarized in Table 2. This

behaviour can be explained by the pore-blockage of the support after the reaction. Both temperatures showed similar results indicating that increasing the reaction temperature from 225°C to 325°C causes only minor changes to the catalyst surface area.

Table 2.BET surface area for the fresh and used methanol catalysts reacted at 225°C, 325°C and S/C of 1.7.

	Surface area (m^2/g)		
	fresh	**reacted at 225°C**	**reacted at 325°C**
10%Ni	122	119	117
10%Cu	120	96	98
7%Cu-3%Ni	125	94	94
5%Cu-5%Ni	128	90	89
3%Cu-7%Ni	125	94	95

3.2.3 TPR

The hydrogen uptake for the catalyst reduction is shown in Fig.7. The 10%Cu catalyst is reduced at 250°C. The wide peak at this reduction temperature is attributed to the dispersion of CuO over the Al_2O_3 support and the amount of hydrogen required reacting with reducible particles. The finding agrees with that found by Jones and Hagelin [29]. The 10%Ni catalyst revealed multi broad peaks at 400°C and 650°C. Both peaks are attributed to a range of interactions between NiO and the Al_2O_3 support. The reduction temperature at 400°C corresponds to weak interaction between NiO and Al_2O_3 support and the reduction temperature at 650°C is likely to be related to a strong interaction of NiO and Al_2O_3[30-32]. The TPR profile of the bimetallic Ni-Cu catalysts (Fig. 7) shows three hydrogen uptake peaks. The first obtained peak on 7%Cu-3%Ni and 5%Cu-5%Ni showed high hydrogen uptake compared to 7%Ni-3%Cu. This indicates that a high area of hydrogen uptake peaks is related to the amount of reducible species of CuO, which increases in samples containing higher percentages of Cu. Therefore, the first sharp peak is associated with pure CuO and is shifted compared to the monotype Cu catalysts due to different amounts of Cu loadings and the rate of hydrogen uptake on CuO species. The broad peak in the middle (350°C for 7%Cu-3%Ni, 380°C for 5%Cu-5%Ni, 425°C for 7%Ni-3%Cu) of the TPR trace for the bimetallic catalyst can be associated with NiCuO interaction with support which was used to determine the reduction temperature for the subsequent reaction study. In addition, it can also indicate a weak interaction of NiO with support. The last peak is related to a strong interaction of NiO with the support. The difference in the position of reduction peaksreported here is related to the fact that the temperature of the reduction peaks strongly depend on the particle dimension and the interaction strength between metal particles and the support[15].

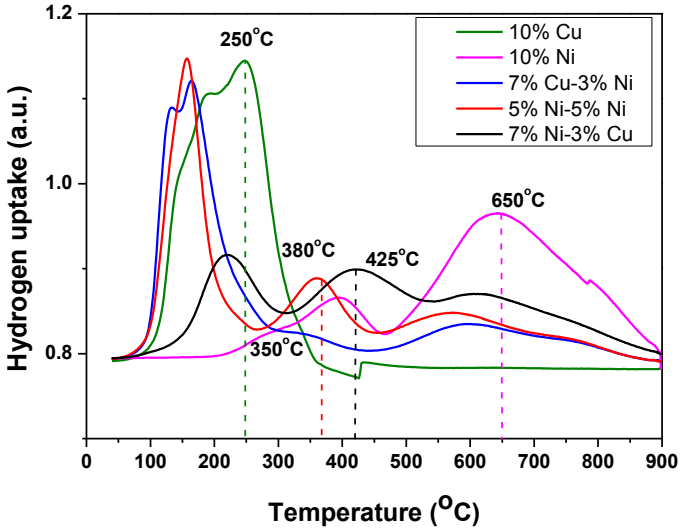

Fig.7. TPR for the prepared catalysts.

3.2.4 XRD

The XRD pattern performed for the unused catalyst is shown in Fig.8a. The monotype catalyst suggested the existence of NiO in the 10%Ni catalyst sample at (2θ = 45°, 60°) with the average crystallite diameter calculated by Scherrer's equation ($L = \frac{K\lambda}{\beta \cos\theta}$) of 17.8 nm. The monotype catalyst of 10%Cu showed XRD patterns of CuO spectra at (2θ = 35°,39°,50°,55°,58°,61°,75°) and the average crystallite size of CuO was 17.9 nm. On the other hand, the bimetallic catalysts indicated the formation of NiO, CuO phases and $Ni_xCu_{1-x}O$ phase at (2θ = 36°). For instance, the crystallite diameter size of $Ni_xCu1_{-x}O$ was 16.7 nm.

The XRD patterns for the used catalysts operated at 225°C and 325°C and S/C of 1.7 are shown in Fig.8b and Fig.8c, respectively. The XRD patterns showed that no metal oxide phase was detected, except for aluminates related to the support material. The monotype catalyst 10%Cu showed XRD patterns of Cu metals at 2θ = 44°, 50° and 72° and the average crystallite size of Cu was 18.1 nm. The bimetallic used catalysts showed patterns related to metallic Ni and metallic Cu and for Ni-Cu. The average crystallite size of bimetallic catalysts is 16.8 nm at 2θ = 37°. The formation of a Ni-Cu alloy reported in the literature depends on the amount of Ni contents, indicating the Ni rich alloy or Cu rich alloy catalyst [20, 33]. The rich Ni alloy phase or rich Cu alloy phase determines the reaction paths. For instance, a dominant decomposition reaction occurred with 7%Ni-3%Cu over the metallic phase of Ni

which was concluded from the high concentration of CO produced at 225-275°C. However, 7%Cu-3%Ni showed a dominant decomposition reaction over the metallic phase of Cu as a large amount of CO was produced at 300-325°C. The XRD patterns for used catalyst operated at 225°C and 325°C showed similar patterns, such that the effects of reaction temperature on the metal phase cannot be deduced. However, the XRD patterns displayed less diffuse and sharper patterns for the catalysts reacted at 325°C than 225°C. This would be possible due to crystallite growth with increasing the reaction temperature.

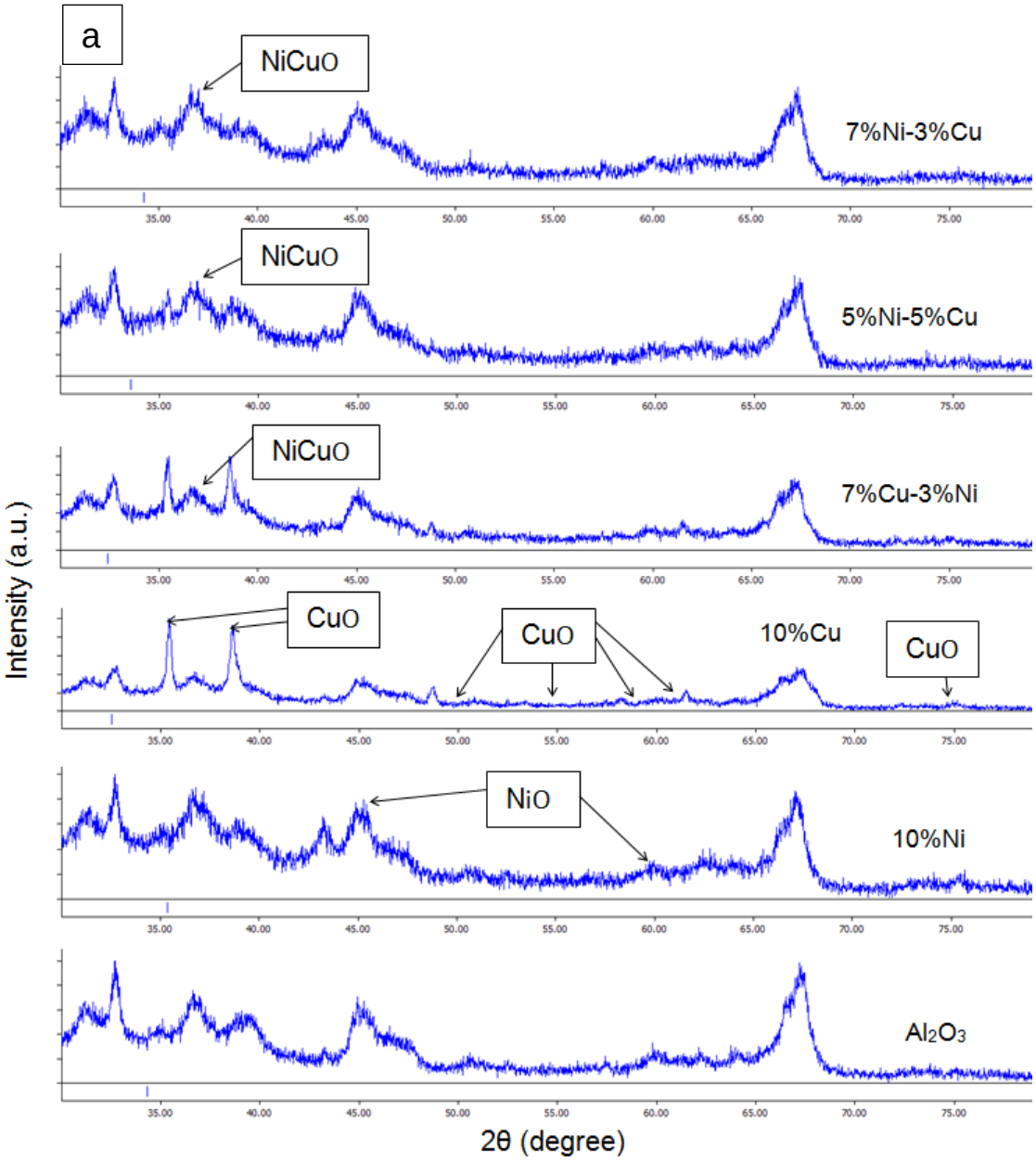
a
NiCuO
7%Ni-3%Cu
NiCuO
5%Ni-5%Cu
NiCuO
7%Cu-3%Ni
CuO
CuO
10%Cu
CuO
NiO
10%Ni
Al2O3
Intensity (a.u.)
2θ (degree)
35.00
40.00
45.00
50.00
55.00
60.00
65.00
70.00
75.00

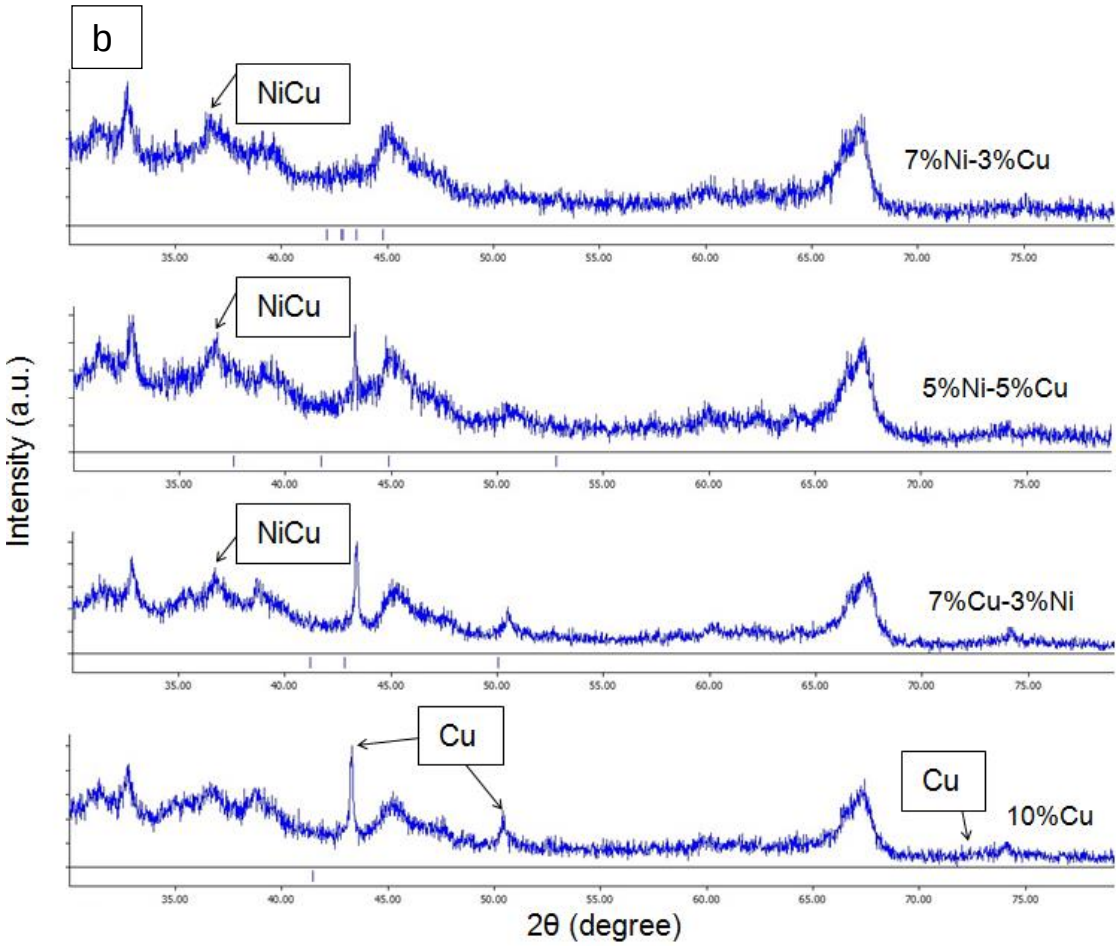
b
NiCu
7%Ni-3%Cu
NiCu
5%Ni-5%Cu
NiCu
7%Cu-3%Ni
Cu
Cu
10%Cu
Intensity (a.u.)
2θ (degree)
35.00
40.00
45.00
50.00
55.00
60.00
65.00
70.00
75.00

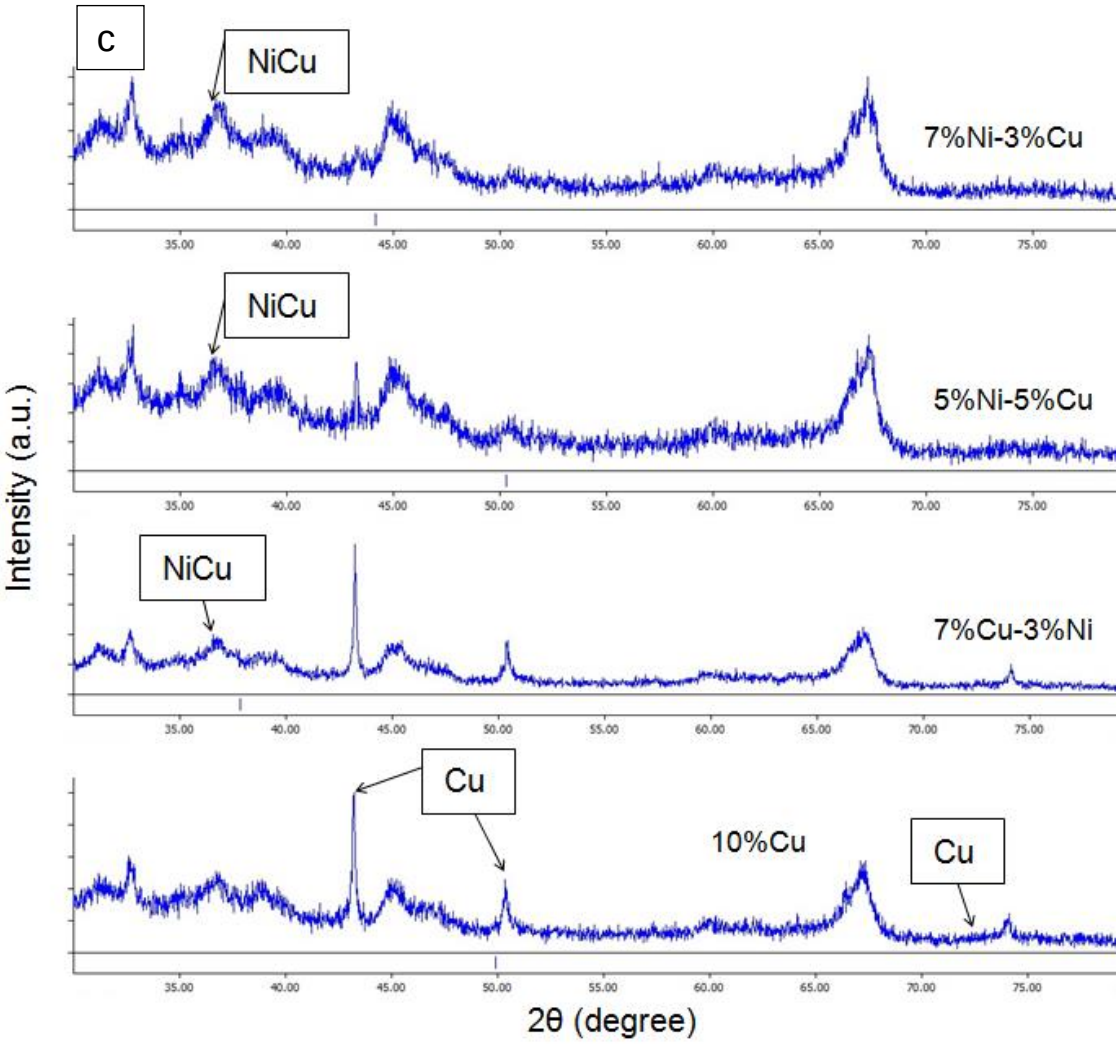

*Fig. 8.*XRD patterns for fresh and used catalysts: a) fresh catalysts, b) used catalysts reacted at 225°C and S/C of 1.7 and c) used catalysts reacted at 325°C and S/C of 1.7.

3.2.5TGA

Table 3 presents the results of carbon selectivity (Eq.4) for the reacted catalysts. The carbon formation depends on the catalyst composition and reaction temperature [34]. The bimetallic rich Ni catalyst (5%Cu-5%Ni and 3%Cu-7%Ni) reacted at temperature 300°C showed less carbon deposition than 10%Cu and 7%Cu-3%Ni. On other hand, 7%Cu-3%Ni and 3%Cu-7%Ni showed less carbon deposition than 10%Cu reacted at temperature 250°C. The 10%Cu catalyst produced less carbon than 7%Cu-3%Ni and 5%Cu-5%Ni reacted at temperature 225°C. It was found that the dominant reaction

over Ni metals is methanol decomposition reaction. Therefore, an abundance of CO was noticed in the reformate gases with Ni containing catalysts compared to the gas composition from the 10%Cu catalyst. Previous work in an alloying effects claimed that Cu surface energy is lower compared with Ni and a small size mismatch between Cu and Ni allows Cu atoms to segregate on the Ni-Cu surface causing the Ni sites responsible for carbon formation [35]. The Cu species doesn't easily dissociate CO at low temperature [20, 36-38]. The current results of carbon formation can't deduce whether the Cu alloying with Ni has any strong evidence that carbon selectivity can be reduced during methanol steam reforming for current operation conditions.

Table 3. Carbon selectivity on the used methanol catalysts reacted at 225-325°C and S/C of 1.7.

	10%Cu	**7%Cu-3%Ni**	**5%Cu-5%Ni**	**3%Cu-7%Ni**
T (°C)	Sel_C (%)	Sel_C (%)	Sel_C (%)	Sel_C (%)
225	0.3	0.9	0.6	0.3
250	1.4	0.2	1.1	0.3
275	0.8	0.8	0.8	1.4
300	1.1	1.4	0.3	0.3
325	1.8	1.3	2.3	1.2

4. Conclusions

The increasing Ni metals content had a positive effect on methanol conversion and showed a high methanol conversion at 300-325°C. The methanol conversion was high for 5%Cu-5%Ni and 7%Cu-3%Ni (98.5%) at 325°C which could possibly be explained by the active decomposition reaction. The current work also revealed that bimetallic catalytic performance affected the reformate compositions compared to the monometallic catalysts trying to investigate if the metallic and alloy phase of metals will affect the catalytic performance toward the syngas production in methanol steam reforming process. The influence of increase the Ni content had shown an increase in CO and decrease in CO_2 yields. This confirmed that Ni rich catalysts (more than 5wt%) is favourable for methanol decomposition reaction. The bimetallic catalyst did not produce any CH_4, revealing that Cu alloying in Ni catalyst had an inhibiting effect for CO and/or CO_2 hydrogenation. The results showed that Cu-based catalysts had good activity for the water gas shift reaction, and had no methanation activity. The existence of single Ni catalyst in the reactor promoted CH_4 formation by CO and CO_2 hydrogenation. The reaction over physical mixture of catalyst showed less CO and more CO_2 than the bimetallic

catalytic system. This indicated that the 10 wt % Cu catalyst in the physical mixture of catalyst controls the high activity of the water gas shift reaction. The current results of carbon formation can't deduce whether the Cu alloying with Ni has any strong evidence that carbon selectivity can be reduced during methanol steam reforming for current operation conditions.

References:

[1] Little A. Multi-fuel reformers for fuel cells used in transportation. Phase 1: Multi-fuel reformers. Cambridge1994.
[2] Sofoklis SM. Hydrogen storage and compression: Institution of Engineering and Technology.
[3] Gkanas EI, Khzouz M, Panagakos G, Statheros T, Mihalakakou G, Siasos GI, et al. Hydrogenation behavior in rectangular metal hydride tanks under effective heat management processes for green building applications. Energy.142:518-30.
[4] Lwin Y, Daud WRW, Mohamad AB, Yaakob Z. Hydrogen production from steam-methanol reforming: Thermodynamic analysis. International Journal of Hydrogen Energy. 2000;25:47-53.
[5] Kolb G. Fuel Processing For Fuel Cells. Weinheim: Wiley-VCH; 2008.
[6] Peppley BA, Amphlett JC, Kearns LM, Mann RF. Methanol-steam reforming on $Cu/ZnO/Al_2O_3$ catalysts. Part 2. A comprehensive kinetic model. Applied Catalysis A: General. 1999;179:31-49.
[7] Peppley BA, Amphlett JC, Kearns LM, Mann RF. Methanol-steam reforming on $Cu/ZnO/Al_2O_3$. Part 1: the reaction network. Applied Catalysis A: General. 1999;179:21-9.
[8] Agarwal V, Patel S, Pant KK. H_2 production by steam reforming of methanol over $Cu/ZnO/Al_2O_3$ catalysts: transient deactivation kinetics modeling. Applied Catalysis A: General. 2005;279:155-64.
[9] Purnama H, Ressler T, Jentoft RE, Soerijanto H, Schlögl R, Schomäcker R. CO formation/selectivity for steam reforming of methanol with a commercial $CuO/ZnO/Al_2O_3$ catalyst. Applied Catalysis A: General. 2004;259:83-94.
[10] Basile A, Parmaliana A, Tosti S, Iulianelli A, Gallucci F, Espro C, et al. Hydrogen production by methanol steam reforming carried out in membrane reactor on Cu/Zn/Mg-based catalyst. Catalysis Today. 2008;137:17-22.
[11] Amphlett JC, Creber KAM, Davis JM, Mann RF, Peppley BA, Stokes DM. Hydrogen production by steam reforming of methanol for polymer electrolyte fuel cells. International Journal of Hydrogen Energy. 1994;19:131-7.
[12] Peters R, Düsterwald HG, Höhlein B. Investigation of a methanol reformer concept considering the particular impact of dynamics and long-term stability for use in a fuel-cell-powered passenger car. Journal of Power Sources. 2000;86:507-14.
[13] Wu H, La Parola V, Pantaleo G, Puleo F, Venezia A, Liotta L. Ni-Based Catalysts for Low Temperature Methane Steam Reforming: Recent Results on Ni-Au and Comparison with Other Bi-Metallic Systems. Catalysts. 2013;3:563-83.
[14] Angeli SD, Monteleone G, Giaconia A, Lemonidou AA. State of the art catalysts for CH_4 steam reforming at low temperature. International Journal of Hydrogen Energy. 2014;39:1979-97.
[15] Khzouz M, Wood J, Kendall K, Bujalski W. Characterization of Ni–Cu-based catalysts for multi-fuel steam reformer. International Journal of Low-Carbon Technologies. 2012;7:55-9.
[16] Carrero A, Calles JA, Vizcaíno AJ. Hydrogen production by ethanol steam reforming over Cu-Ni/SBA-15 supported catalysts prepared by direct synthesis and impregnation. Applied Catalysis A: General. 2007;327:82-94.
[17] Vizcaíno AJ, Carrero A, Calles JA. Hydrogen production by ethanol steam reforming over Cu–Ni supported catalysts. International Journal of Hydrogen Energy. 2007;32:1450-61.
[18] Mariño F, Boveri M, Baronetti G, Laborde M. Hydrogen production from steam reforming of bioethanol using $Cu/Ni/K/\gamma\text{-}Al_2O_3$ catalysts. Effect of Ni. International Journal of Hydrogen Energy. 2001;26:665-8.
[19] Liao P-H, Yang H-M. Preparation of catalyst Ni–Cu/CNTs by chemical reduction with formaldehyde for steam reforming of methanol. Catalysis Letters. 2008;121:274-82.
[20] De Rogatis L, Montini T, Lorenzut B, Fornasiero P. Ni_xCu_y/Al_2O_3 based catalysts for hydrogen production. Energy & Environmental Science. 2008;1:501-9.

[21] Khzouz M, Wood J, Pollet B, Bujalski W. Characterization and activity test of commercial Ni/Al_2O_3, $Cu/ZnO/Al_2O_3$ and prepared $Ni–Cu/Al_2O_3$ catalysts for hydrogen production from methane and methanol fuels. International Journal of Hydrogen Energy. 2013;38:1664-75.
[22] Brunauer S, Emmett PH, Teller E. Adsorption of gases in multimolecular layers. Contribution from the bureau of chemistry and soils and george washington university. 1938.
[23] Khzouz M, Gkanas E. Experimental and Numerical Study of Low Temperature Methane Steam Reforming for Hydrogen Production. Catalysts.8:5.
[24] NETZSCH. Operating instructions TG 209 F1 iris. Gemany: NETZSCH-Gerätebau GmbH.
[25] Post E. Principles of TG, DSC, STA and EGA. Germany: NETZSCH; 2009.
[26] Echegoyen Y, Suelves I, Lázaro MJ, Sanjuán ML, Moliner R. Thermo catalytic decomposition of methane over Ni–Mg and Ni–Cu–Mg catalysts: Effect of catalyst preparation method. Applied Catalysis A: General. 2007;333:229-37.
[27] Lázaro MJ, Echegoyen Y, Suelves I, Palacios JM, Moliner R. Decomposition of methane over Ni-SiO_2 and Ni-Cu-SiO_2 catalysts: Effect of catalyst preparation method. Applied Catalysis A: General. 2007;329:22-9.
[28] Twigg MV, Spencer MS. Deactivation of copper metal catalysts for methanol decomposition, methanol steam reforming and methanol synthesis. Topics in Catalysis. 2003;22:191-203.
[29] Jones SD, Hagelin-Weaver HE. Steam reforming of methanol over CeO_2- and ZrO_2-promoted Cu-ZnO catalysts supported on nanoparticle Al_2O_3. Applied Catalysis B: Environmental. 2009;90:195-204.
[30] De Rogatis L, Montini T, Cognigni A, Olivi L, Fornasiero P. Methane partial oxidation on NiCu-based catalysts. Catalysis Today. 2009;145:176-85.
[31] Roh H-S, Jun K-W, Dong W-S, Chang J-S, Park S-E, Joe Y-I. Highly active and stable Ni/Ce–ZrO_2 catalyst for H_2 production from methane. Journal of Molecular Catalysis A: Chemical. 2002;181:137-42.
[32] Ye J, Li Z, Duan H, Liu Y. Lanthanum modified $Ni/\gamma\text{-}Al_2O_3$ catalysts for partial oxidation of methane. Journal of Rare Earths. 2006;24:302-8.
[33] Lee J-H, Lee E-G, Joo O-S, Jung K-D. Stabilization of Ni/Al_2O_3 catalyst by Cu addition for CO_2 reforming of methane. Applied Catalysis A: General. 2004;269:1-6.
[34] Bartholomew CH. Mechanisms of catalyst deactivation. Applied Catalysis A: General. 2001;212:17-60.
[35] Ferrando R, Jellinek J, Johnston RL. Nanoalloys: From theory to applications of alloy clusters and nanoparticles. Chemical Reviews. 2008;108:845-910.
[36] Ponec V. Selectivity in the syngas reactions: The role of supports and promoters in the activation of CO and in the stabilization of intermediates: Elsevier; 1991.
[37] Schwank J. Bimetallic catalysts for CO activation. Studies in Surface Science and Catalysis: Elsevier; 1991. p. 225-64.
[38] Ponec V, Bond GC. Catalysis by metals and alloys: Elsevier; 1995.